Regenerative Therapy 24 (2023) 190–200

Contents lists available at ScienceDirect

Regenerative Therapy

journal homepage: http://www.elsevier.com/locate/reth

Original Article

Association with cationized gelatin nanospheres enhances cell internalization of mitochondria efficiency

Wenxuan Yang, Satoshi Abe, Yasuhiko Tabata*

Laboratory of Biomaterials, Institute for Life and Medical Sciences, Kyoto University, Kawahara-cho Shogoin, Sakyo-ku, Kyoto, 606-8507, Japan

ARTICLE INFO

Article history:
Received 30 April 2023
Received in revised form
11 June 2023
Accepted 24 June 2023

Keywords:
Mitochondria internalization
Cationized gelatin
Nanospheres
ROS
ATP

ABSTRACT

The objective of this study is to confirm the methodological feasibility of cationized gelatin nanospheres (cGNS) to enhance the internalization efficiency of mitochondria (Mt) isolated to cells for their increasing functions. The cGNS were simply associated on the surface of Mt by the electrostatic interaction. Different sizes of cGNS were used to allow Mt to associate on the Mt surface (Mt-cGNS). As a control, cationized gelatin (cG) was used to modify the Mt surface (Mt-cG). The Mt-cG and Mt-cGNS prepared were cultured with H9c2 cells to examine their internalization. The internalization efficiency significantly increased by utilizing cGNS. However, there was no significant difference in the internalization efficiency among cGNS with different sizes. After incubation of Mt, Mt-cG, and Mt-cGNS, the superoxide amount and ATP generation were evaluated. Significantly lower superoxide amount and higher ATP amount were observed for the Mt-cGNS group compared with those of non-modified Mt group. It is conceivable that cGNS enhance the cellular internalization of Mt, leading to an improve mitochondrial functions in the recipient cells. In conclusion, cGNS are promising to improve the efficacy in mitochondria internalization.

1. Introduction

Mitochondria (Mt) are known as the "powerhouse" of cells. They are involved in multiple important cell functions, such as respiration, biosynthesis, apoptosis, reactive oxygen species (ROS) homeostasis, and metabolism. It has been reported that the mitochondrial dysfunction often results in many diseases, including diabetes, neurodegenerative diseases, cardiovascular diseases, ischemia, spinal cord injury, cancer, and senescence [1–4]. Based on this finding, it is clinically important to find an effective therapeutic way to rescue the mitochondrial dysfunction.

Recently, the intracellular mitochondrial transfer is observed under physiological conditions [5–7]. The intact healthy mitochondria are transferred from donated cells to recipient cells through four routes, tunneling nanotubes (TNT), extracellular vesicles (EV), gap junction channels (GCJs), and cell fusion [6,8]. It is well recognized that the mitochondria transferred in the recipient cells not only contribute to damaged tissue repair, but also the inflammation regulation. This phenomenon gives an idea to treat the mitochondrial dysfunction through the mitochondrial internalization, which means the transplantation of healthy exogenous mitochondria to the mitochondria-defected cells.

As one simple way of the mitochondria internalization, isolated Mt are incubated with the recipient cells to allow them to internalize to the cells. However, due to the electrostatic repulsion between the cell and mitochondria membranes, it is technically difficult to internalize Mt at a high efficiency. Several methods have been reported to solve this problem. For example, a simple method named Mito-Ception is reported [9]. The mixture of cells and isolated Mt is centrifuged, leading to an improved cellular internalization of Mt in vitro, irrespective of the cell type. A Mito-Punch system using a pressure-driven way to achieve highly efficient and quick cellular internalization of Mt is also reported [10]. However, there still remain some problems that need to be improved. The methods based on the physical forces often cause the cell membrane opening which threatens the cell viability. In addition, the methods are technically challenging for the Mt internalization in vivo.

* Corresponding author. Fax: +81 75 751 4646.
E-mail address: yasuhiko@infront.kyoto-u.ac.jp (Y. Tabata).

Peer review under responsibility of the Japanese Society for Regenerative Medicine.

https://doi.org/10.1016/j.reth.2023.06.011

From the viewpoint of drug delivery system (DDS) technology, several methods to internalize nuclear acids, proteins, and molecular probes into cells at a high efficiency, have been developed. The electroporation can assist the cellular internalization of drugs by puncturing a cell membrane with electrical stimulation [11]. Viral vectors are used for the highly efficient transfection of pDNA [12]. Lipid or polymer nanoparticles incorporating drugs have been developed for safe pDNA delivery [13,14]. However, Mt are quite different from the drugs used in terms of the size. In this connection, it is difficult to apply the conventional methods for the cellular internalization of Mt without modification. Therefore, it is necessary to develop techniques suitable for the efficient cellular internalization of Mt.

Modification of Mt surface seems to be essential to increase the cellular internalization of Mt. Mt modification with cell penetrating peptides (CPP) is one of the trials to enhance the Mt internalization. After 48 h incubation, the CPP-modified Mt were delivered to recipient cells, resulting in the recovery of respiration [15]. On the other hand, cationic lipids are utilized for the Mt surface modification. The coating with an artificial DOTAP/DOPE membrane permitted Mt to improve the cellular internalization, leading to an enhanced neuroprotection [16].

Gelatin is a well-known biocompatible and biodegradable material. It is derived from collagen and has been widely applied for food, medicine, and clinical uses, which demonstrates the potential to be a safety carrier material. Cationized gelatin (cG) was successfully synthesized by chemically introducing spermine to the amino groups of gelatin [17]. With the positive charge, the hydrogel of cationized gelatin can incorporate the nucleic acids of siRNA [18] and pDNA [17], to achieves the high efficiency of intracellular delivery.

The objective of this study is to evaluate whether or not cGNS are effective in enhancing the cellular internalization of Mt. When the cGNS were mixed with Mt for their simple association and cultured with H9c2 cells for 6 h, the cellular interaction was evaluated to compare with that of Mt alone and Mt associated with cG. The Mt functions of scavenging ROS and producing ATP were assessed before and after the cells cultured with Mt for internalization.

2. Materials and methods

2.1. Preparation of cationized gelatin (cG) and cationized gelatin nanospheres (cGNS)

According to the preparation procedure previously reported [19] the carboxyl groups of gelatin were chemically converted by introducing amino groups to allow gelatin to cationize. Spermine was added at a molar ratio of 50 to the carboxyl groups of gelatin into 50 ml of double-distilled water (DDW) containing 2.0 g of gelatin (isoelectric point (pI) = 9.0, weight-averaged molecular weight = 99,000, derived from pig skin, Nitta Gelatin Inc., Osaka, Japan.). Immediately after that, the solution pH was adjusted to 5.0 by adding 11 M HCl aqueous solution. Next, 1-ethyl-3-(3-dimethyl aminopropyl) carbodiimide (EDC) was added at a molar ratio of 3 to the carboxyl groups of gelatin. The reaction mixture was agitated at 37 °C for 18 h, and then dialyzed against DDW for 3 days at room temperature. The dialyzed solution was freeze-dried to obtain cationized gelatin (cG). To determine the percentage of amino groups introduced into gelatin, the conventional 2,4,6-trinitrobenzene sulfonic acid (TNBS, Wako Pure Chemical Industries, Ltd., Osaka, Japan) method was performed. The percentage was 44.5 mol% per the carboxyl groups of gelatin.

cGNS were prepared by the conventional coacervation method [18]. In brief, 1.25 ml of cationized gelatin aqueous solution (2.5, 3.25, 6.25, and 10 wt%) was warmed up to 40 °C. Next, 5 ml of acetone was added to the solution, and the coacervate was formed. Then, glutaraldehyde (25 wt%, 20 μl) was added to chemically crosslink cGNS for 6 h. For the blocking of aldehyde groups unreacted, 2 ml of glycine aqueous solution (0.5 M) was added. The resulting solution was agitated overnight at 40 °C and the residual acetone was evaporated. cGNS were collected by the centrifugation of 250,000 g for 30 min at 25 °C and resuspended in DDW. cGNS were resuspended in 10 mM phosphate buffered-saline solution (PBS, pH7.4), and the apparent size of nanospheres was measured by dynamic light scattering (DLS, Zetasizer Nano-ZS, Malvern Instruments Ltd., Worcestershire, UK). On the other hand, cGNS were resuspended in 10 mM phosphate buffer solution (PB, pH7.4), and the zeta potential was measured by electrophoresis light scattering (ELS, Zetasizer Nano-ZS, Malvern Instruments Ltd., Worcestershire, UK).

2.2. Cell culture

H9c2 cardiomyoblasts were obtained from the American Type Culture Collection (ATCC, Rockville, MD). The H9c2 cells were maintained in Dulbecco's Modified Eagle Medium (Thermo Fisher Scientific, Inc., Massachusetts) supplemented with 10 vol% fetal bovine serum and 1 vol% penicillin/streptomycin mixture. The cells were incubated at 37 °C in a humidified atmosphere with 5% CO^2. Stably Green fluorescent protein (GFP) expressing H9c2 cells (GFP-H9c2) were generated to visualize the mitochondria isolated. A plasmid Su9- EGFP was kindly provided by Dr. Ishihara [20] (Department of Biological Sciences, Graduate School of Science, Osaka University). According to the manufacturer's protocol, the pDNA was transfected by using Lipofectamine® 3000 (Thermo Fisher Scientific, Inc., Massachusetts). After the transfection, cells were cultured in the medium containing a selective agent, G418, for 3 weeks. Finally, GFP-expressing cells were selected and collected by Cell Sorter MA900 (Sony Inc., Tokyo, Japan). The Su9-EGFP-expressing H9c2 cells were stained with the mitochondria-specific dye MitoBright LT Deep Red (Dojindo, Kumamoto, Japan) or Hoechst 33,258 (Thermo Fisher Scientific, Inc., Massachusetts). The expression of GFP in H9c2 cells was observed by a fluorescent microscopy BZ-X700 (KEYENCE Co., Ltd., Osaka, Japan).

2.3. Isolation of mitochondria (Mt)

Mitochondria were isolated from H9c2 or GFP-H9c2 cells. After disrupting cells through a 27- gauge needle, the isolation was conducted based on the research procedure of Maeda et al. [21]. Briefly, cells were ruptured by 20 strokes using a syringe with 27-gauge needle in homogenization buffer [HB; 20 mM HEPES-KOH (pH 7.4), 220 mM mannitol 70 mM sucrose 100 μM PMSF (Phenylmethylsulfonyl fluoride). The homogenate was centrifuged at 400 g at 4 °C for 5 min to remove unbroken cells, and the supernatant was further centrifuged at 6000 g for 5 min to pellet the isolated Mt-enriched fraction (Mt fraction). The mitochondria isolated from H9c2 cells are defined as Mt, while the mitochondria isolated from GFP-H9c2 are defined as Mt-GFP. The supernatant was collected as a cytosolic fraction. The amount of protein in each fraction was measured by Pierce™ BCA Protein Assay Kit (Thermo Fisher Scientific, Inc., Massachusetts). The purity of mitochondria obtained was confirmed by detecting a mitochondrial-specific protein, COXIV, and a cytosol specific protein, α-tubulin as comparison.

2.4. Preparation of Mt associated with cG and cGNS

The cG and cGNS (5 μl, 1 mg/ml) were added to 95 μl suspension of Mt (15 μg) and gently mixed, followed by incubation for 10 min

on ice. The zeta potential was measured by ELS (Zetasizer NanoZS, Malvern Instruments Ltd., Worcestershire, UK). In addition, Mt labeled with MitoBright LT DeepRed and cGNS-labeled with FITC were mixed to allow to associate to each other. The co-localization was observed by a fluorescent microscopy BZ-X700 (KEYENCE Co., Ltd., Osaka, Japan).

2.5. Confocal microscopy to evaluate cellular internalization of Mt

H9c2 cells were seeded in a glass bottom dishes (diameter = 35 mm, Matsunami Glass Industries Ltd., Tokyo, Japan) (1×10^5 cells/well). After cultured overnight, cells were stained with 100 nM of MitoTracker™ Red CMRos (Thermo Fisher Scientific, Inc., Massachusetts) for 30 min. And then, the stained cells were incubated with Mt-GFP-cGNS for 6 h. The z-stack images were taken by a confocal laser scanning microscope (FV1000D, Olympus, Japan).

2.6. Western blotting to evaluate cellular internalization of Mt

H9c2 cells were seeded in each well of 6 multi-well culture plates (1×10^5 cells/well). After cultured overnight, cells were incubated with Mt-GFP, Mt-GFP-cG, and Mt-GFP-cGNS for 6 h. And then, cells were trypsinized and centrifuged (400 g, 3 min, 25 °C) to collect the cells. The pellets were mixed with the Laemmli buffer (Bio-Rad Laboratories, Inc., Hercules, CA, USA), to prepare the cell lysate. The amount of GFP in the cell lysates was quantified by the western blotting. In brief, samples were loaded on Any kD™ Mini-PROTEAN TGX™ Precast Gels (Bio-Rad Laboratories, Inc., Hercules, CA, USA) and electrophoretically run at 0.02 A for 15 min and 0.04 A for 40 min. Then, the samples were transferred onto a polyvinylidene difluoride (PVDF) membrane and blocked with the blocking solution (Immuno Block™, KAC Co. Ltd., Kyoto, Japan) for 1 h and washed 3 times with Tris-buffered saline solution containing 1 vol% Tween-20 (TBST). For detection, the primary antibodies were added and the membranes were incubated overnight at 4 °C. The blots were washed 3 times with TBST before incubation with the HRP-conjugated secondary antibody for 1 h at room temperature. Finally, membranes were washed 3 times with TBST and detected using a PierceTM ECL Plus Western Blotting Substrate (Thermo Fisher Inc., Waltham, MA, USA) with a chemiluminescence imaging system LAS-4000 (FUJIFILM Co., Tokyo, Japan). The efficiency was calculated as the ratio of the amount of GFP contained in each sample to that of GFP in the sample cultured with Mt-GFP. The antibodies used in this study are summarized in Table 1.

2.7. Cytochrome c reduction assay

H9c2 cells (5×10^3 cells/well) were seeded in each well of 96 multi-well culture plate (Corning Inc., Corning, NY, USA) and incubated overnight. After incubation with Mt, Mt-cGNS (50, 100, 200, and 400) for 6 h, cells were treated with 5 μM menadione and 0.5 mg/ml cytochrome *c* in Hank's Balanced Salt Solution (HBSS) for 1 h. The absorption at 550 nm was measured by a multi-mode microplate reader (SpectraMax i3x, Molecular Devices Japan Co., Ltd., Tokyo, Japan).

2.8. ATP assay

To determine the activity of isolated Mt, isolated Mt were separated into three group. One group was associated with cGNS to prepare Mt-cGNS, while another group was treated with 10 μM of oligomycin for 20 min. The triplicate samples of Mt, Mt-cGNS, and oligomycin-treated Mt were added to each well of 96 multi-well white wall plate (SUMITOMO BAKELITE Co. Ltd. Japan) followed by adding same volume of CellTiter-Glo® 2.0 reagent (Promega Corporation, Madison, USA). After mixing on the shaker for 5 min covered with a aluminum foil, the luminescent signal was stabilized for 10 min and record by Multi-mode Microplate Reader (SpectraMax i3x, Molecular Devices Japan Co., Ltd., Tokyo, Japan).

H9c2 cells (5×10^3 cells/well) were seeded in each well of 96 multi-well plate (Corning Inc., Corning, NY, USA) and incubated overnight. After incubation with Mt, Mt-cGNS (50, 100, 200, and 400) for 6 h, the cells were washed with PBS two times. Then, 50 μl PBS was added to each well, followed by adding 50 μl of CellTiter-Glo® 2.0 reagent into each well. After mixing on the shaker for 5 min covered with a aluminum foil, 70 μl solution in each well was removed to each well of 96 multi-well white wall plate to decrease the crosstalk of the luminescent signal during detection. After stabilization of the luminescent signal at room temperature for 10 min, the luminescence was recorded by Multi-mode Microplate Reader.

2.9. Statistical analysis

The data were expressed as the mean ± standard deviation (SD). All the statistical analysis was performed by using an unpaired *t*-test with two tails. Difference with $p < 0.05$ was considered to be significant.

3. Results

3.1. Characterization of Su-EGFP-expressing H9c2 cells

Fig. 1 shows the fluorescent images of Su9-EGFP-expressing H9c2 cells. The red fluorescence of MitoBright LT DeepRed shows the mitochondria location. The green fluorescence of GFP was observed, which is corresponding with that of mitochondria. In addition, the fluorescence of GFP was detected around nuclei (stained with Hoechst 33,258).

3.2. Characterization of mitochondria isolated

Fig. 2 shows the western blotting result of different cell fractions obtained during the mitochondria isolation. The COXIV of a mitochondria-specific protein was not detected in the cytosol fraction, while small amount of a cytosol-specific protein, α-tublin was detected in the mitochondria fraction. The purity of

Table 1
Antibodies used for western blotting analysis.

Antibody	Source	Product number	Dilution
Mouse monoclonal anti-COXIV	Abcam (Cambridge, UK)	ab14744	1:1000
Rabbit polyclonal anti-α-Tubulin	Cell Signaling Technology Japan, K.K. (Tokyo, Japan)	2144S	1:1000
Rabbit polyclonal anti-GFP	Abcam	ab290	1:3500
Rabbit monoclonal anti-β-Actin	Cell Signaling Technology	4970S	1:1400
HRP-linked goat anti-rabbit IgG	Cell Signaling Technology	7074S	1:2000
HRP-linked horse anti-mouse IgG	Cell Signaling Technology	7076S	1:2000

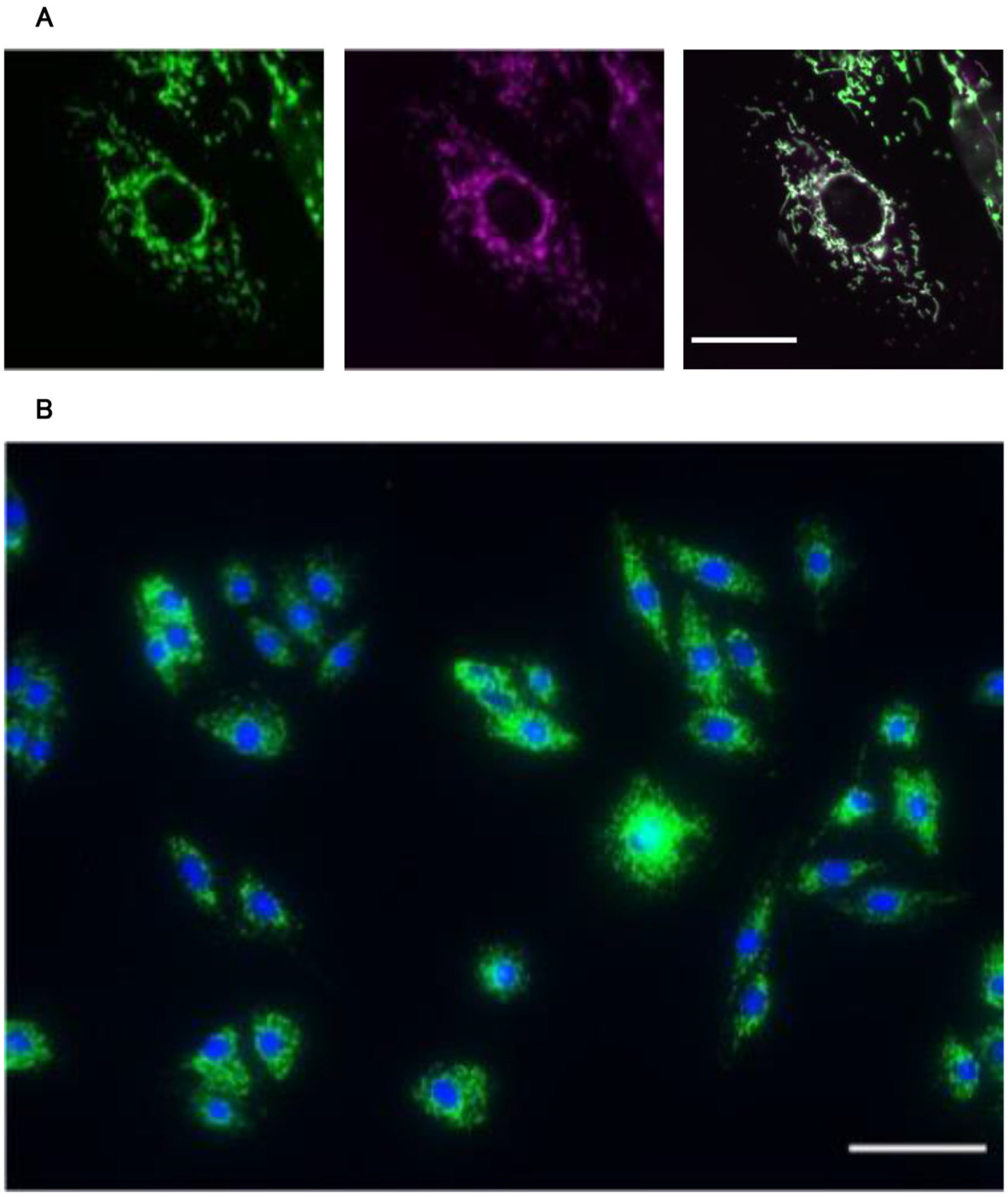

Fig. 1. A. fluorescent images of Su9-EGFP-expressing H9c2 cells stained with MitoBright LT Deep Red: GFP (left), MitoBright LT Deep Red (middle), and co-localization (right) images. Scale bar is 30 μm. B. fluorescent images of Su9-EGFP-expressing H9c2 cells stained with Hoechst 33,258 Blue: nuclei. Green: Su9-EGFP. Scale bar is 60 μm.

mitochondria isolated was confirmed. On the other hand, the ATP amount of isolated mitochondria increased proportionately with an increase in the mitochondria amount (Fig. 3).

3.3. Characterization of mitochondria associated with or without cGNS

Table 2 summarizes the size and potential of cGNS used. The apparent size of cGNS increased with an increase of cG concentration. The value of zeta potential was positive for any size of cGNS. Table 3 shows the zeta potentials of Mt-cGNS. After association with cGNS, the zeta potentials of Mt increased. The mitochondria labeled with MitoBright LT DeepRed was co-localized with FITC labeled cGNS, irrespective of the cGNS size (Fig. 4). In addition, there was no difference between Mt and Mt-cGNS in terms of ATP amount (Fig. 5).

3.4. Cellular internalization efficiency of Mt associated with or without cG and cGNS

Mt-GFP were detected in every stack of recipient H9c2 cells after 6 h co-incubation (Fig. 6). Fig. 7 shows the efficiency of cellular

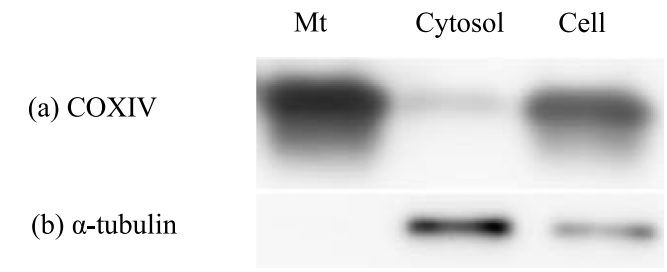

Fig. 2. Western blotting images of different fractions obtained by the conventional differential centrifugation: Mt fraction (Mt), cytosolic fraction (Cytosol), and total cell extracts (Cell). Anti-COXIV (a) and anti-α-tubulin antibodies (b) are used as the markers of Mt and cytosol, respectively.

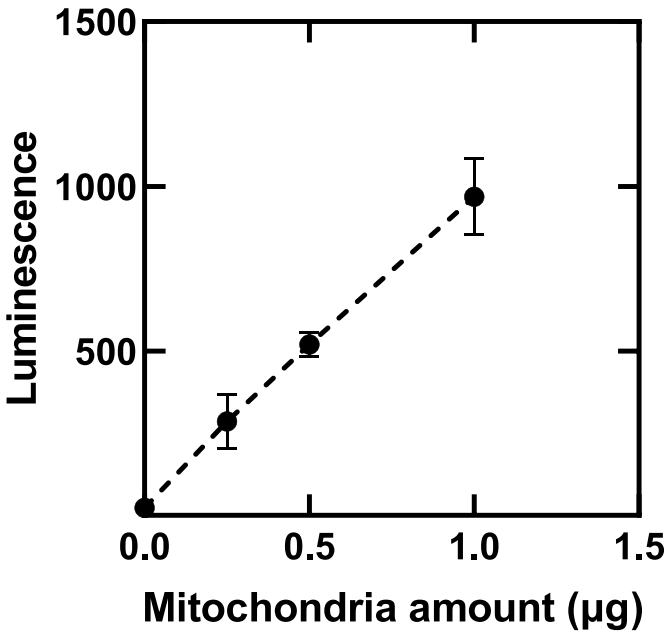

Fig. 3. Relationship between mitochondria amount and the luminescence.

Significantly higher amount of GFP was observed for the Mt-cGNS groups compared with that of only Mt group and Mt-cG groups. However, there was no significant difference in the internalization efficiency among any sizes of cGNS.

3.5. Functions of cells internalized with Mt with or without cG and cGNS

Fig. 8 shows the amount of superoxide anions. In comparison with the untreated cells, cells treated with menadione generated a higher amount of superoxide. The amount of superoxide generated was reduced for the cells incubated with the Mt to a significant great extent compared with those without treatment. In addition, the amount in cells incubated with the Mt-cGNS was significantly less than that of cells incubated with Mt and Mt-cG. No significantly higher reducing effect than Mt was observed for cells incubated with Mt-cG, which is different from the Mt-cGNS.

The ATP amount in the cells incubated with Mt-cGNS was higher than that of no treated cells (Fig. 9). Significantly higher ATP amount was observed after applying 7.5 and 15 μg Mt-cGNS compared with that of no treated cells. On the contrary, there was no significant difference between non-treated and 30 μg Mt-cGNS-cultured cells.

4. Discussion

In present study, we demonstrates the methodological feasibility of a cationized material, cGNS, to enhance the cellular internalization efficiency of Mt isolated into cells to increase cell functions. cG and cGNS with different sizes were prepared according to the method previously reported [18]. The Mt were isolated from H9c2 cells while the purity and activity of Mt isolated were experimentally confirmed. The increased zeta potential of Mt by mixing cG and cGNS revealed the successful association of cG and cGNS with Mt. Significant higher internalization efficiency was observed after the internalization of Mt-cGNS compared with that of Mt-cG. In addition, the internalization of Mt-cGNS allowed cells to improve the metabolic functions in terms of a decreased superoxide amount and increased ATP production. Mitochondrial dysfunction is a hallmark of many types of diseases. An artificial mitochondria transfer gives a new strategy to rescue the mitochondrial dysfunction. However, the low transfer efficiency is still challenging for developing this research field. So far, the technology to enhance the mitochondria internalization efficiency can be divided into two categories. The first category is using physical force to allow more mitochondria to internalize into recipient cells, for instance, Mito-Ception [9], Mito-Punch [10], and Magneto-mitotransfer [22]. However, they are challenging for Mt internalization in vivo. Another category is Mt surface modification. Cell-penetrating peptides [15], cationic ligand conjugated-polymer [23], and cationic lipid modification [16] has been reported can enhance the Mt internalization efficiency.

Table 2
Physicochemical properties of cGNS prepared.

Code	The concentration of cG added (wt%)	Apparent size (nm)	Zeta potential (mV)
cGNS(50)	2.50	151.8 ± 0.12[a)]	6.21 ± 0.71[a)]
cGNS(100)	3.75	194.4 ± 0.39a)	8.75 ± 0.64a)
cGNS(200)	6.25	197.0 ± 2.26a)	7.51 ± 0.52a)
cGNS(400)	10.0	403.0 ± 4.97a)	6.99 ± 0.21a)

[a)] Mean ± standard deviation.

Table 3
Zeta potentials of Mt and Mt associated with cG and cGNS.

Sample	Zeta potential (mV)
Mt	−26.3 ± 1.79[a)]
Mt-cG	−9.09 ± 0.714
Mt-cGNS(50)	−14.4 ± 1.59
Mt-cGNS(100)	−20.4 ± 0.41
Mt-cGNS(200)	−20.4 ± 0.49
Mt-cGNS(400)	−20.7 ± 0.62

[a)] Mean ± standard deviation.

internalization of Mt and Mt associated with cG and cGNS. The Mt-GFP internalization was observed in all the Mt-treated groups, indicating the successful cellular internalization of exogenous Mt.

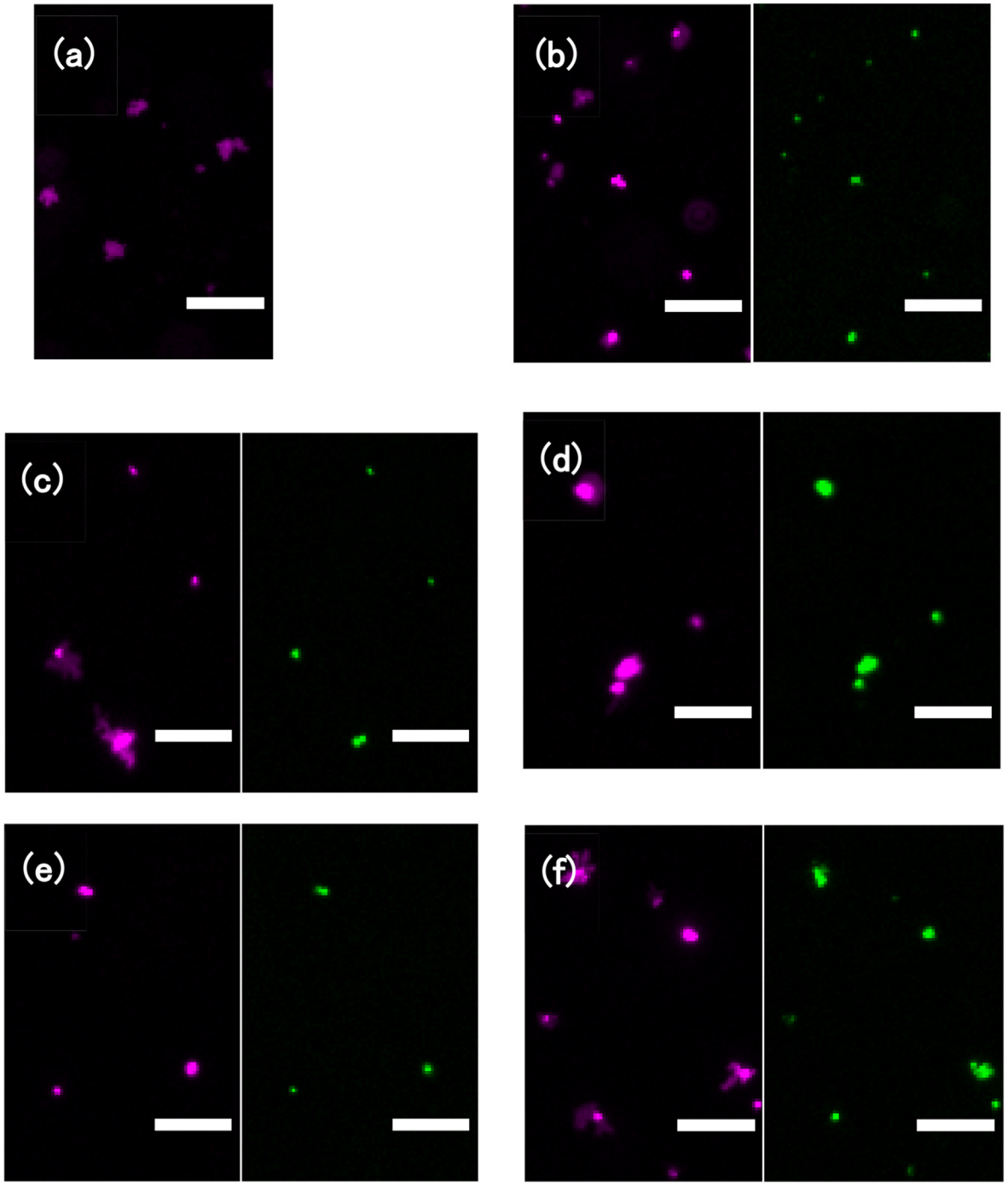

Fig. 4. Fluorescent microscopic images of Mt (a), Mt-cG (b), Mt-cGNS(50) (c), Mt-cGNS(100) (d), Mt-cGNS(200) (e), and Mt-cGNS(400) (f). Magenta: Mt. Green: cG or cGNS. Scale bar is 5 μm.

Comparing with other studies, just by a mixing procedure, both cG and cGNS can be easily modified on Mt surface by the electrostatic interaction. In addition, it is reported that spermine with secondary amino groups shows a buffering effect to enhance the endosomal escape [24]. It is conceivable that cG and cGNS with spermine play a role in the pH-buffering effect to allow Mt to escape from the endosome. The biodegradability of cGNS was confirmed in a previous study, but should be optimized for the Mt internalization in the future.

To evaluate the cellular internalization efficiency of mitochondria isolated, GFP-expressing H9c2 cells were prepared as the exogenous mitochondria source. Although a fluorescence dye is often used to label mitochondria, mitochondria are dynamically fussed and fissured, leading to loss of fluorescence signal [25–27]. In addition, a long time incubation might lead to the fluorescence detaching from mitochondria. As one trial to tackle this issue, mitochondria genetically labeled with GFP were prepared by transfecting plasmid to H9c2 cells. The fluorescence of Su9-EGFP was observed around each nucleus ubiquitously, indicating the successful selection of stable Su9-EGFP-expressing cells (Fig. 1).

It is well recognized that the surface potential of Mt was negative, while that of cGNS was positive (Tables 2 and 3). After Mt were

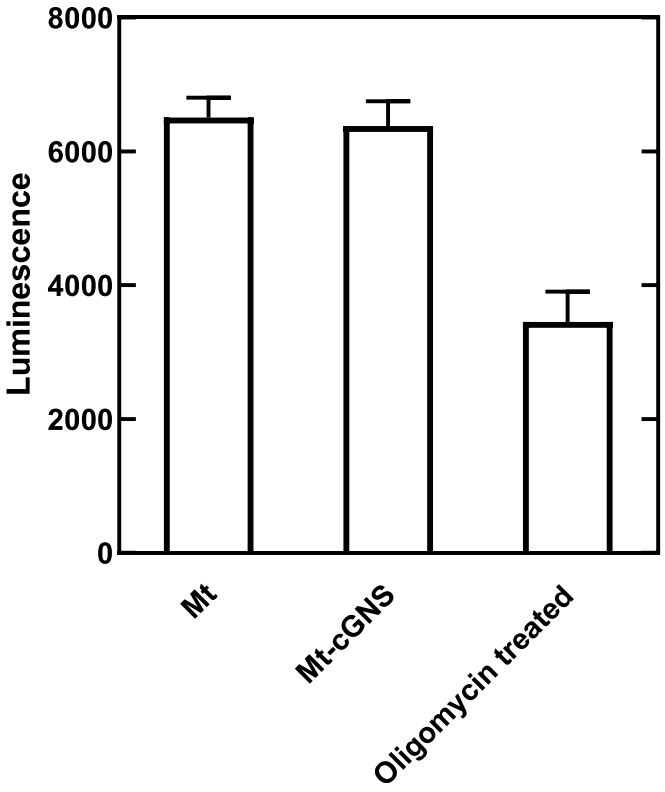

Fig. 5. Luminescence of Mt isolated with and without cGNS coating. Mt treated with oligomycin are used as a positive control.

associated with cG or cGNS, their surface potential increased (Table 3). In addition, it is reported that the size of mitochondria is around 1 μm. However, the sizes of cGNS used in this study ranged from 50 to 400 nm. It is highly conceivable that cG and cGNS were attached to the Mt surface through the electrostatic interaction force, leading to a reduced Mt zeta potential. It should be noted that the association of cGNS did not affect the mitochondrial function (Fig. 5).(See Tables 4 and 5)

After culture for 6 h, Mt-cGNS were internalized into cells (Fig. 6). When cells were incubated with Mt-cGNS, the amount of Mt internalized was about 6 times higher than that incubated with Mt alone. It is reported that the cellular internalization efficiency of Mt modified with cell penetrating peptides (CPP) was 2 or 3 times higher than that of non-modified Mt [15,28]. Indeed, it is difficult to compare our result with that result because different cells and evaluation methods are used. However, it may be concluded that Mt-cGNS were a promising system for the enhanced cellular internalization of Mt.

A higher internalization efficiency of Mt-cGNS was observed than that of Mt-cG. This can be explained in terms of cationic charges flexibility. It is possible that the cG molecule of water-soluble polymer is flexible and tightly interacts with the negative surface of Mt. On the contrary, the positive charge of cGNS is rather fixed and less flexible because the charge is localized on the surface of nanospheres. It is likely that in addition to the positive charges on one side of nanospheres interacting with Mt, the positive charges on the other side remain to interact with the recipient cells, leading to an enhanced internalization of Mt into the cells.

No significant difference in the internalization efficiency was observed among different sizes of cGNS as the Mt carrier. However the internalization efficiency of Mt-cGNS(400) was relatively lower than that of other sizes of cGNS. The reason is still unclear. It might be possible that the larger size of cGNS is easier to contact with many Mt, to form an increased Mt aggregation, leading to a reduced Mt internalization. It is reported that isolated Mt are intracellularly internalized by macropinocytosis [29,30]. It is well known that macropinosomes range from 0.2 μm to 5 μm. Therefore, the Mt aggregation would affect the cellular internalization of Mt,

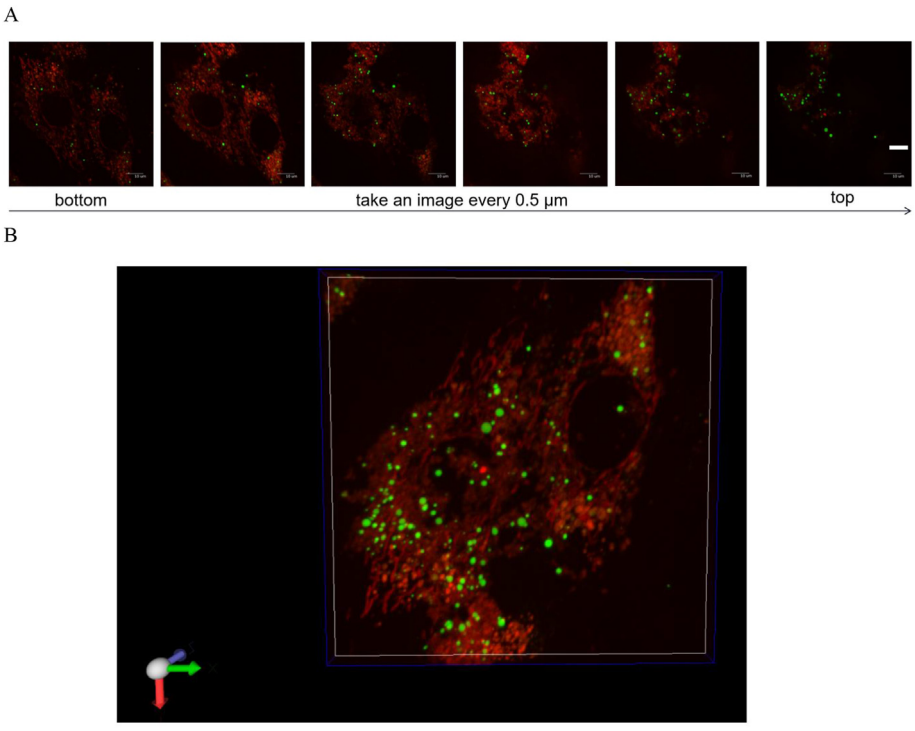

Fig. 6. A. Fluorescence images of H9c2 cells 6 h after incubation with Mt-GFP-cGNS at different z-positions. Red: endogenous mitochondria. Green: exogenous mitochondria. Scale bar: 1 μm. B. A 3D image of H9c2 cells incubated with Mt-GFP-cGNS.

A

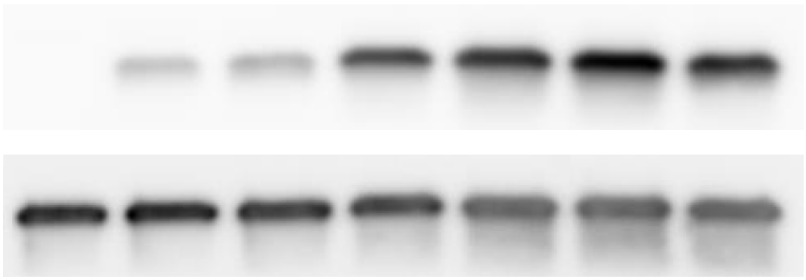

Mt	-	+	+	+	+	+	+
Carrier material	-	-	cG	cGNS (50)	cGNS (100)	cGNS (200)	cGNS (400)

B

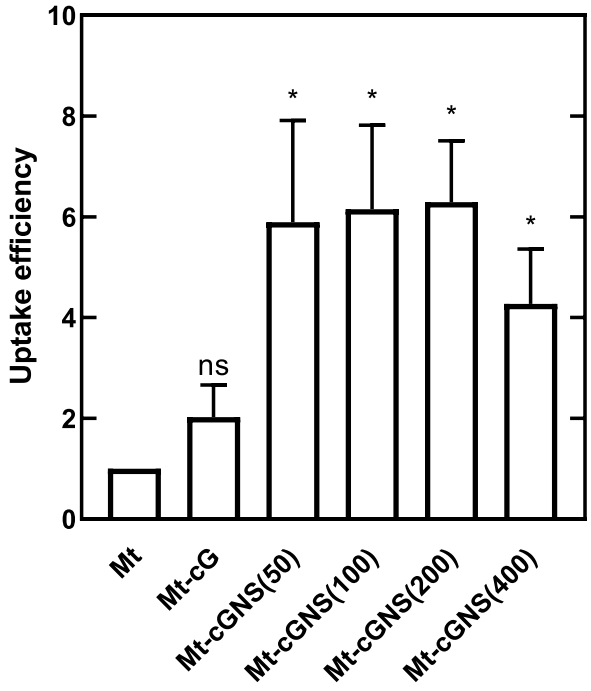

Fig. 7. A. Western blotting image of cell lysates after cellular internalization of Mt and Mt associated with cG and cGNS. B. Efficiency of cellular internalization of Mt and Mt associated with cG and cGNS. The value for the Mt group is 1. *, $p < 0.05$; significant difference from the Mt group, ns; not significant.

resulting in the relatively lower internalization efficiency of Mt-cGNS(400). Further investigation is needed to make clear the internalization mechanism.

There have been reported on two different fates of exogenous mitochondria in recipient cells. The mitochondria without any modification might fail in endosomal escape and finally degrade. In the case of spontaneous mitochondria transfer, mitochondria are degraded after internalized into other cells [31,32]. This mitochondrial transcellular degradation is considered as a more advanced method to degrade mitochondria and keep the mitochondrial homeostasis in recipient cells. On the other hand, in the case of artificial transfer of mitochondria, it is demonstrated that most of exogenous mitochondria can effectively fuse with the endogenous mitochondrial network, while some of mitochondria are destined to degrade [33]. In our study, the amino groups are chemically introduced in cG and cGNS by reacting with spermine. It is recognized that the secondary amino groups show the pH buffering effect, which may lead to the endosomal escape of Mt-cG and Mt-cGNS. The cG and cGNS will gradually be degraded while the exogenous mitochondria will fuse into original mitochondria network. The fusion of mitochondria enlarges and rearranges the component inside the original mitochondria network, promoting the weak mitochondria to be excluded from the new mitochondrial network which result in an increase of mitochondrial function [5,34–36]. After the mitochondria transfer, the total volume of mitochondria and metabolic fitness of chimeric antigen receptor

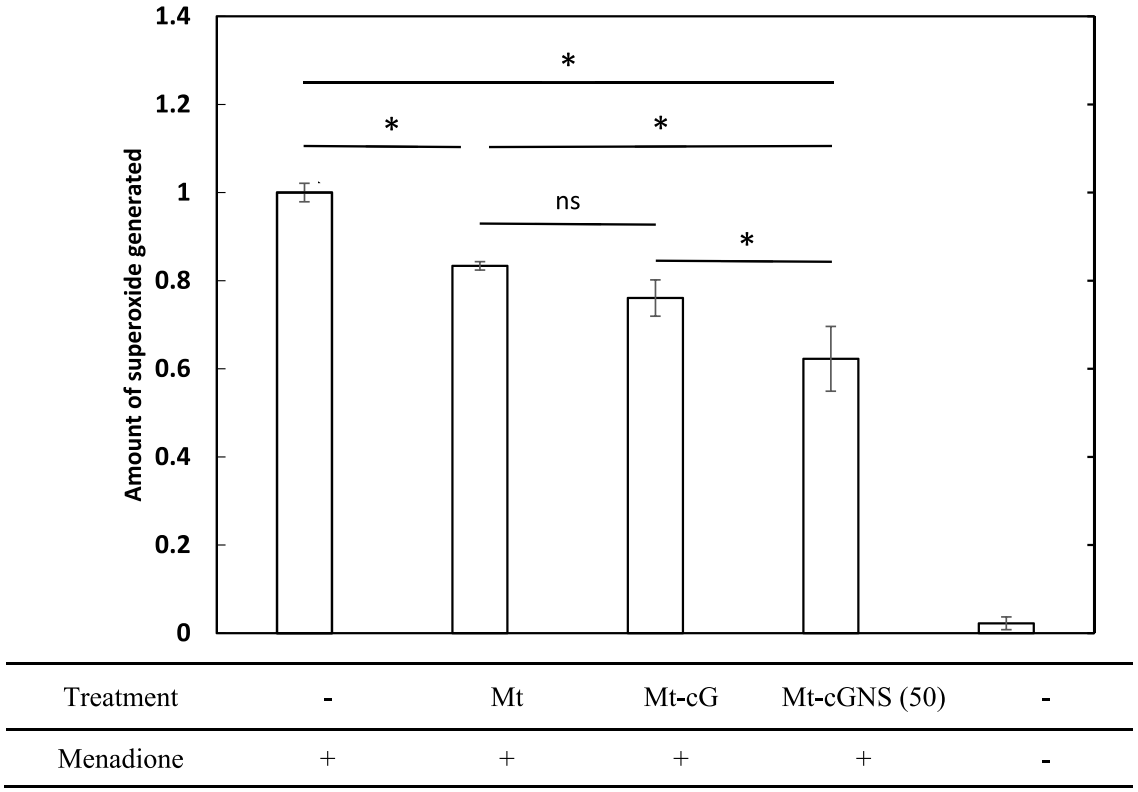

Fig. 8. The amount of superoxide generated from cells by the menadione treatment. The value of cells treated with menadione is 1. *, $p < 0.05$; significant difference between the two groups, ns; not significant.

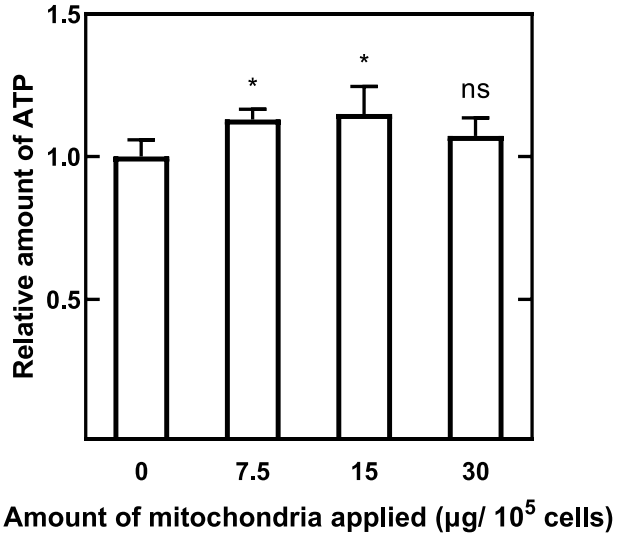

Fig. 9. ATP amount of cells 6 h incubated with 7.5, 15, and 30 μg Mt associated with cGNS. *, $p < 0.05$; significant difference from the value of mitochondria amount 0 μg, ns; not significant.

Table 5
Treatments of samples.

Treatment	–	Mt	Mt-cG	Mt-cGNS (50)	–
Menadione	+	+	+	+	–

(CAR) T-cell are improved [37]. Coincidentally, the internalization of exogenous mitochondria into adipose-derived mesenchymal stem cells switches the metabolism method from OXPHOS to glycolysis [38]. In this study, the recipient cells used are healthy H9c2 cells. Therefore, an enhancement of metabolic abilities after internalizing mitochondria will be expected.

In this study, as two functions of mitochondria, the ability to maintain the homeostasis of ROS, and the ability to produce ATP. Mitochondria are known as the main source of reactive oxygen species (ROS) [39]. Nearly 90% of ROS are generated in the mitochondrial electron transportation chain. During the process of oxidative phosphorylation, an electron transfer and the interaction with molecular oxygen to form superoxide mainly in mitochondria complex I and III. On the other hand, mitochondria have an antioxidant enzyme system to eliminate ROS. Superoxide dismutase (SOD) and catalase convert superoxide to hydrogen peroxide in mitochondrial intermembrane space and mitochondrial matrix, respectively. Non-enzymatic antioxidants, such as ubiquinol,

Table 4
Treatments of samples.

Mt	–	+	+	+	+	+	+
Carrier material	–	–	cG	cGNS (50)	cGNS (100)	cGNS (200)	cGNS (400)

vitamin C, and uric acid, also assist to eliminate ROS [40]. By keeping the balance between the production and elimination of ROS, the oxidative stress does not occur in healthy cells. Menadione is often used to prepare the oxidative stress and post-ischaemic damage models by generating superoxide anion [41,42]. After treated with menadione, cells generated superoxide, and the amount of superoxide was significantly higher than that of cells incubated with Mt, Mt-cG, and Mt-cGNS (Fig. 8). This result indicates that the internalization of Mt assisted to scavenge ROS, which is well corresponding with previous reports [43]. Zhang et al. demonstrate that via increasing the ATP supplement and reducing the subsequent activation of apoptosis signaling pathway, the mitochondrial internalization can accelerate ROS scavenging [44]. After the Mt internalization, the level of catalase antioxidant enzyme and the SOD2 protein expression were found upregulated, which contributes to the inhibition of ROS production [45,46]. Combined with the previous result (Fig. 7), we can say with certainty that a higher amount of Mt internalized into cells leads to a higher ability to scavenge superoxide.

ATP generation is one of the most essential functions of mitochondria. Around 95% of ATP is produced by mitochondria. It is likely that the internalization of healthy mitochondria gives more ATP producer to cells to assist ATP production. After mitochondria internalization, the ATP production significantly increased compared with that of non-treated cells (Fig. 9). It is possible to consider that exogenous Mt function to enlarge the original mitochondrial network and consequently promote the mitochondrial ability of ATP production. However, this enhancement of ATP production was not in a dose-dependent manner. Assuming 100% applied Mt were internalized, these results indicated that there is a preferable range of exogenous Mt doses for internalization. It has been reported that as few as 100 cells were sufficient to rescue 1 cell clone via intracellular mitochondrial transfer [5]. According to this report, Chang and his group report that the applied Mt amount which lower than 21 $\mu g/10^5$ cells or higher than 105 $\mu g/10^5$ cells was ineffective for restoring the mitochondria membrane potential in MERRF cybrid cells under peptide-mediated mitochondrial delivery [47]. Another research demonstrate that the neuroprotection of oxygen-glucose deprivation cells peaked under the treatment with an Mt dose of 50 $\mu g/10^5$ cells in vitro [16]. In this study, the Mt doses applied were 7.5, 15, and 30 $\mu g/10^5$ cells. However, the rescue effect of Mt internalization with the doses of 7.5 and 15 $\mu g/10^5$ cells was still observed in this study (Fig. 9). It might be due to the recipient cells being healthy which do not require much more Mt supplement. Meanwhile, the enhancement of Mt internalization using cGNS as a carrier might also contribute to this effect. For further research to understand the Mt internalization mechanism and optimize the dose of Mt to apply, Mt-deficient cells should be used as the recipient cells.

Mitophagy plays an important role in controlling the quality of mitochondria. Inducing mitophagy is one of the methods to cure the dysfunction mitochondria. It is reported that the presence of healthy mitochondria is required to proceed this process [48]. cGNS used as a potential tool to deliver healthy mitochondria also utilize the carrier of drug release. The controlled release mitophagy-inducing drugs may be attraction for this research area. Further investigation will be proceeded to make clear underlying mechanism.

5. Conclusion

Mitochondria internalization is an innovative strategy for the mitochondria dysfunction treatment. This study demonstrate that cGNS enabled to enhance the intracellular uptake of exogenous Mt, leading to the recovery of Mt functions. By the cGNS association with Mt, the internalization efficiency of Mt significantly increased. With an increased amount of Mt internalizing into cells, the cells functions of scavenging ROS and generating ATP were enhanced. In conclusion, cGNS are potential carriers to improve the therapeutic efficacy of mitochondria internalization.

Declaration of competing interest

The authors declare the following financial interests/personal relationships which may be considered as potential competing interests:Abe Satoshi reports equipment, drugs, or supplies was provided by Osaka University.

Acknowledgment

The plasmid Su9- EGFP was non-finacially supported by Osaka University for research usage.

References

[1] Ballinger SW. Mitochondrial dysfunction in cardiovascular disease. Free Radic Biol Med 2005;38(10):1278–95.
[2] V. Sorrentino, K.J. Menzies, J. Auwerx, Repairing mitochondrial dysfunction in disease, in: P.A. Insel (Ed.), Annual review of pharmacology and toxicology, Vol vol. 582018, pp. 353-389.
[3] Wang W, Zhao F, Ma X, Perry G, Zhu X. Mitochondria dysfunction in the pathogenesis of Alzheimer's disease: recent advances. Mol Neurodegener 2020;15(1):1–22.
[4] Moon HE, Paek SH. Mitochondrial dysfunction in Parkinson's disease. Experimental neurobiology 2015;24(2):103.
[5] Lin H-Y, Liou C-W, Chen S-D, Hsu T-Y, Chuang J-H, Wang P-W, et al. Mitochondrial transfer from Wharton's jelly-derived mesenchymal stem cells to mitochondria-defective cells recaptures impaired mitochondrial function. Mitochondrion 2015;22:31–44.
[6] Liu D, Gao Y, Liu J, Huang Y, Yin J, Feng Y, et al. Intercellular mitochondrial transfer as a means of tissue revitalization. Signal Transduct Targeted Ther 2021;6(1):65.
[7] Spees JL, Olson SD, Whitney MJ, Prockop DJ. Mitochondrial transfer between cells can rescue aerobic respiration. Proceedings of the National Academy of Sciences of the United States of America 2006;103(5):1283–8.
[8] Liu Z, Sun Y, Qi Z, Cao L, Ding S. Mitochondrial transfer/transplantation: an emerging therapeutic approach for multiple diseases. Cell Biosci 2022;12(1):1–29.
[9] Caicedo A, Fritz V, Brondello JM, Ayala M, Dennemont I, Abdellaoui N, et al. MitoCeption as a new tool to assess the effects of mesenchymal stem/stromal cell mitochondria on cancer cell metabolism and function. Sci Rep 2015;5:9073.
[10] Sercel AJ, Napior AJ, Patananan AN, Wu T-H, Chiou P-Y, Teitell MA. Generating stable isolated mitochondrial recipient clones in mammalian cells using MitoPunch mitochondrial transfer. STAR protocols 2021;2(4):100850.
[11] Kim TK, Eberwine JH. Mammalian cell transfection: the present and the future. Anal Bioanal Chem 2010;397(8):3173–8.
[12] Shi J, Ma Y, Zhu J, Chen Y, Sun Y, Yao Y, et al. A review on electroporation-based intracellular delivery. Molecules 2018;23(11):3044.
[13] Kulkarni JA, Cullis PR, Van Der Meel R. Lipid nanoparticles enabling gene therapies: from concepts to clinical utility. Nucleic Acid Therapeut 2018;28(3):146–57.
[14] Rothenfluh DA, Bermudez H, O'Neil CP, Hubbell JA. Biofunctional polymer nanoparticles for intra-articular targeting and retention in cartilage. Nat Mater 2008;7(3):248–54.
[15] Chang JC, Hoel F, Liu KH, Wei YH, Cheng FC, Kuo SJ, et al. Peptide-mediated delivery of donor mitochondria improves mitochondrial function and cell viability in human cybrid cells with the MELAS A3243G mutation. Sci Rep 2017;7(1):10710.
[16] Nakano T, Nakamura Y, Park J-H, Tanaka M, Hayakawa K. Mitochondrial surface coating with artificial lipid membrane improves the transfer efficacy. Communications Biology 2022;5(1):745.
[17] Fukunaka Y, Iwanaga K, Morimoto K, Kakemi M, Tabata Y. Controlled release of plasmid DNA from cationized gelatin hydrogels based on hydrogel degradation. J Contr Release 2002;80(1–3):333–43.
[18] Ishikawa H, Nakamura Y, Jo J-i, Tabata Y. Gelatin nanospheres incorporating siRNA for controlled intracellular release. Biomaterials 2012;33(35):9097–104.
[19] Kushibiki T, Tomoshige R, Iwanaga K, Kakemi M, Tabata Y. In Vitro transfection of plasmid DNA by cationized gelatin prepared from different amine compounds. J Biomater Sci Polym Ed 2006;17(6):645–58.
[20] Eura Y, Ishihara N, Yokota S, Mihara K. Two mitofusin proteins, mammalian homologues of FZO, with distinct functions are both required for mitochondrial fusion. The Journal of Biochemistry 2003;134(3):333–44.
[21] Maeda H, Kami D, Maeda R, Murata Y, Jo Ji, Kitani T, et al. TAT-dextran–mediated mitochondrial transfer enhances recovery from models of

reperfusion injury in cultured cardiomyocytes. J Cell Mol Med 2020;24(9):5007–20.
[22] Macheiner T, Fengler VHI, Agreiter M, Eisenberg T, Madeo F, Kolb D, et al. Magnetomitotransfer: an efficient way for direct mitochondria transfer into cultured human cells. Sci Rep 2016;6(1):35571.
[23] Wu S, Zhang A, Li S, Chatterjee S, Qi R, Segura-Ibarra V, et al. Polymer functionalization of isolated mitochondria for cellular transplantation and metabolic phenotype alteration. Adv Sci 2018;5(3):1700530.
[24] Jo J-i, Nagane K, Yamamoto M, Tabata Y. Effect of amine type on the expression of plasmid DNA by cationized dextran. J Biomater Sci Polym Ed 2010;21(2):225–36.
[25] Patel SP, Michael FM, Arif Khan M, Duggan B, Wyse S, Darby DR, et al. Erodible thermogelling hydrogels for localized mitochondrial transplantation to the spinal cord. Mitochondrion 2022;64:145–55.
[26] Gollihue JL, Patel SP, Eldahan KC, Cox DH, Donahue RR, Taylor BK, et al. Effects of mitochondrial transplantation on bioenergetics, cellular incorporation, and functional recovery after spinal cord injury. J Neurotrauma 2018;35(15):1800–18.
[27] Gollihue JL, Patel SP, Mashburn C, Eldahan KC, Sullivan PG, Rabchevsky AG. Optimization of mitochondrial isolation techniques for intraspinal transplantation procedures. J Neurosci Methods 2017;287:1–12.
[28] Chang J-C, Liu K-H, Li Y-C, Kou S-J, Wei Y-H, Chuang C-S, et al. Functional recovery of human cells harbouring the mitochondrial DNA mutation MERRF A8344G via peptide-mediated mitochondrial delivery. Neurosignals 2013;21(3–4):160–73.
[29] Kesner E, Saada-Reich A, Lorberboum-Galski H. Characteristics of mitochondrial transformation into human cells. Sci Rep 2016;6(1):26057.
[30] Kitani T, Kami D, Matoba S, Gojo S. Internalization of isolated functional mitochondria: involvement of macropinocytosis. J Cell Mol Med 2014;18(8):1694–703.
[31] Hayakawa K, Esposito E, Wang X, Terasaki Y, Liu Y, Xing C, et al. Transfer of mitochondria from astrocytes to neurons after stroke. Nature 2016;535(7613):551–5.
[32] Davis C-hO, Kim K-Y, Bushong EA, Mills EA, Boassa D, Shih T, et al. Transcellular degradation of axonal mitochondria. Proc Natl Acad Sci USA 2014;111(26):9633–8.
[33] Cowan DB, Yao R, Thedsanamoorthy JK, Zurakowski D, Del Nido PJ, McCully JD. Transit and integration of extracellular mitochondria in human heart cells. Sci Rep 2017;7(1):17450.
[34] Pacak CA, Preble JM, Kondo H, Seibel P, Levitsky S, Del Nido PJ, et al. Actin-dependent mitochondrial internalization in cardiomyocytes: evidence for rescue of mitochondrial function. Biology open 2015;4(5):622–6.
[35] Santel A, Frank S, Gaume B, Herrler M, Youle RJ, Fuller MT. Mitofusin-1 protein is a generally expressed mediator of mitochondrial fusion in mammalian cells. J Cell Sci 2003;116(13):2763–74.
[36] Archer SL. Mitochondrial dynamics—mitochondrial fission and fusion in human diseases. N Engl J Med 2013;369(23):2236–51.
[37] Harada S, Hashimoto D, Senjo H, Yoneda K, Zhang Z, Chen X, et al. Intercellular mitochondrial transfer enhances metabolic fitness and anti-tumor effects of CAR T cells. Blood 2022;140(Supplement 1):2356–7.
[38] Yao X, Ma Y, Zhou W, Liao Y, Jiang Z, Lin J, et al. In-cytoplasm mitochondrial transplantation for mesenchymal stem cells engineering and tissue regeneration. Bioengineering & Translational Medicine 2022;7(1):e10250.
[39] Murphy MP. How mitochondria produce reactive oxygen species. The Biochemical journal 2009;417(1):1–13.
[40] Ighodaro O, Akinloye O. First line defence antioxidants-superoxide dismutase (SOD), catalase (CAT) and glutathione peroxidase (GPX): their fundamental role in the entire antioxidant defence grid. Alexandria journal of medicine 2018;54(4):287–93.
[41] Chiou T-J, Tzeng W-F. The roles of glutathione and antioxidant enzymes in menadione-induced oxidative stress. Toxicology 2000;154(1–3):75–84.
[42] White EJ, Clark JB. Menadione-treated synaptosomes as a model for post-ischaemic neuronal damage. Biochem J 1988;253(2):425–33.
[43] Emani SM, Piekarski BL, Harrild D, Del Nido PJ, McCully JD. Autologous mitochondrial transplantation for dysfunction after ischemia-reperfusion injury. J Thorac Cardiovasc Surg 2017;154(1):286–9.
[44] Zhang S, Rao S, Yang M, Ma C, Hong F, Yang S. Role of mitochondrial pathways in cell apoptosis during He-patic ischemia/reperfusion injury. Int J Mol Sci 2022;23(4):2357.
[45] Chang J-C, Chang H-S, Wu Y-C, Cheng W-L, Lin T-T, Chang H-J, et al. Mitochondrial transplantation regulates antitumour activity, chemoresistance and mitochondrial dynamics in breast cancer. J Exp Clin Cancer Res 2019;38(1):30.
[46] Konari N, Nagaishi K, Kikuchi S, Fujimiya M. Mitochondria transfer from mesenchymal stem cells structurally and functionally repairs renal proximal tubular epithelial cells in diabetic nephropathy in vivo. Sci Rep 2019;9(1):5184.
[47] Chang J-C, Liu K-H, Chuang C-S, Su H-L, Wei Y-H, Kuo S-J, et al. Treatment of human cells derived from MERRF syndrome by peptide-mediated mitochondrial delivery. Cytotherapy 2013;15(12):1580–96.
[48] Dai Y, Zheng K, Clark J, Swerdlow RH, Pulst SM, Sutton JP, et al. Rapamycin drives selection against a pathogenic heteroplasmic mitochondrial DNA mutation. Hum Mol Genet 2014;23(3):637–47.